I-1. PROJECT RESEARCHES

Project 3

PR3 Project Research on Advances in Isotope-Specific Studies Using Muti-Element Mössbauer Spectroscopy

M. Seto

Institute for Integrated Radiation and Nuclear Science, Kyoto University

OBJECTIVES OF RESEARCH PROJECT:

Mössbauer spectroscopy is effective to extract several information such as electronic states for a specific isotope. The objective of this project research is to progress the investigation in the frontier of the materials science and the development of advanced experimental methods by using multi-element Mössbauer spectroscopy. Promotion of variety of Mössbauer isotope provides more useful and valuable methods in modern materials science even for complicated systems.

In this project research, each group performed their research by specific isotopes:

^{57}Fe in R4P3-1, R4P3-2, R4P3-3, R4P3-4, R4P3-5, R4P3-6

^{61}Ni in R4P3-7

^{197}Au in R4P3-8, R4P3-9

Other developments in R4P3-10, R4P3-11

R4P3-2(H. Fujii) was not performed this year.

MAIN SUBJECTS AND RESULTS OF THIS REPORT:

Main subjects and results are as follows:

(R4P3-1, K. Shinoda) Intensity tensor of Fe^{2+} in the *M1* Site of diopside by single crystal Mössbauer spectroscopy

K. Shinoda *et al.* successfully characterized the intensity tensor of quadrupole doublet of diopside, which is Ca-rich and Fe-poor pyroxene, in a natural mineral by Mössbauer microspectrometer.

(R4P3-3, I. Mashino) Electrical conductivity and the iron valence state of silicate glasses up to Mbar pressures

I. Mashino *et al.* investigated Fe-bearing enstatite glasses with variable amounts of iron components. The Mössbauer spectroscopy at room and low temperatures is used to determine the composition ratio and of Fe^{2+} and Fe^{3+}components.

(R4P3-4, M. Tabuchi) Change in Fe valence state of Fe and Ni substituted Li_2MnO_3 positive electrode material during different synthetic method by ^{57}Fe Mössbauer spectroscopy

M. Tabuchi *et al.* performed ^{57}Fe Mössbauer spectroscopy for several samples of Fe and Ni substituted Li_2MnO_3 electrode materials with different preparation method to improve the electro-chemical performance as positive electrodes in Li-ion batteries.

(R4P3-5, Y. Kamihara) Research on magnetism and electronic phase in a H-doped iron-based superconductor

Y. Kamihara *et al.* prepared iron-based superconductors, H-doped SmFeAsO by high-temperature and high-pressure synthesis and evaluated magnetic properties to investigate the mechanism of superconducting electron pair formation and destruction. The Mössbauer spectroscopy will be performed for this evaluated samples.

(R4P3-6, K. Yonezu) Experimental Preliminary Approach on the Precipitation Mechanism of Banded Iron Formation (BIF): Part 2

K. Yonezu *et al.* performed ^{57}Fe Mössbauer Spectroscopy of silica scales from operating geothermal power plant to understand the banded iron formation mechanism of chemically precipitated sedimentary rock at Precambrian age.

(R4P3-7, T. Kitazawa) ^{61}Ni Mössbauer Spectroscopy for Hofmann-type Supramolecular Bridging Cyanide Complexes

K. Kitase *et al*. synthesized three Hofmann-type Fe-and Ni-contained coordination polymer and investigated them by ^{61}Ni Mössbauer spectroscopy to evaluate the Ni environments in these compounds.

(R4P3-8, H. Ohashi) Chemical species for precursor of supported gold cluster catalysts presumed from Recoil-free fraction in ^{197}Au Mössbauer Spectroscopy

H. Ohashi *et al*. investigated precursor of supported Au cluster and presumed chemical species of the precursor as an analogous complex of $[Au(SH)_2]^-$ by ^{197}Au Mössbauer Spectroscopy.

(R4P3-9, Y. Kobayashi) Recoilless Fraction on ^{197}Au Mössbauer Spectroscopy(2)

Y. Kobayashi *et al.* investigated the evaluation method of the Debye temperature by measuring temperature dependence of Mössbauer spectra for several Au compounds.

(R4P3-10, R. Masuda) EuS property as the energy standard material at ^{151}Eu Mössbauer spectroscopy

R. Masuda *et al*. evaluated the temperature dependence of the isomer shifts of EuS as a Eu^{2+} standard material for ^{151}Eu Mössbauer spectroscopy.

(R4P3-11, S. Kitao) Development of ^{119}Sn Mössbauer Source

S. Kitao *et al*. have attempted to produce a ^{119}Sn Mössbauer source by using $CaSnO_3$ compounds in long-term neutron irradiation.

PR3-1 Intensity tensor for Fe^{2+} at the *M*1 site of diopside by single crystal Mössbauer spectroscopy

K. Shinoda[1], D. Takagi[1], Y. Kobayashi[2]

[1]*Department of Geosciences, Graduate School of Science, Osaka Metropolitan University*
[2]*Institute for Integrated Radiation and Nuclear Science, Kyoto University*

INTRODUCTION: Pyroxene is a major rock-forming mineral and a typical multi-site solid solution. Common chemical formula of natural pyroxene is $(Ca, Fe, Mg)_2 Si_2 O_6$. Occupying sites of divalent cations are the *M*1 and *M*2 sites. In pyroxene, Fe^{2+} in *M*1, Fe^{2+} in *M*2 and Fe^{3+} in *M*1 sites are possible. Fukuyama et al. (2022) emphasized that the intensity tensor for Fe^{2+} at the *M* sites of pyroxene is very important for analyzing Mössbauer spectra of single-crystal pyroxene thin sections, because intensities of a quadrupole doublet of a thin section as a single crystal are asymmetric and vary depending on the angle between the direction of incident γ-rays and the crystallographic orientation. Intensity of quadrupole doublet (I^h / I^{total}) means a ratio between area of the peak of the higher energy (I^h) and total area of the doublet ($I^{total}= I^h + I^l$) (sum of I^h and area of the lower energy (I^l)). Intensity can be calculated from the intensity tensor. Intensity tensors of Ca-rich and Fe-rich pyroxenes (augite and hedenbergite) were revealed by Fukuyama (2022) [1]. However, Intensity tensor of diopside, that is Ca-rich and Fe-poor pyroxene, was not measured. In this study, intensity tensor for Fe^{2+} at the *M*1 site of diopside was measured to confirm compositional dependence of the intensity tensor for Fe^{2+} at the *M*1 site in Ca-rich pyroxene by single crystal Mössbauer spectroscopy.

EXPERIMENTS and RESULTS: Single crystals of diopside from Horado, Seki, Gifu prefecture, Japan were used for this study. Chemical analyses of the diopside indicates the formula $(Ca_{0.97}Fe_{0.06}Mg_{0.94})_{\Sigma 1.97}(Si_{1.99}Al_{0.03})_{\Sigma 2.02}O_6$ by EDS. The molar contents of Mg and Ca were 0.94 and 0.97, respectively. The results suggest that Ca ions almost fully occupy the *M*2 sites and that the Mg ions are not sufficient to occupy the *M*1 sites. Therefore, the major part of the Fe^{2+} ions occupy the *M*1 sites. Three crystallographically oriented thin sections perpendicular to ***a***, ***b*** and ***c*** were prepared by measuring X-ray diffraction using Laue and precession cameras. Eight Mössabuer spectra of oriented thin sections were measured. In this study, Cartesian coordinate (*X Y Z*) is set as *X*//***c****, *Y*//***a***, *Z*//***b***, where ***c**** are reciprocal lattice vectors of diopside. Mössbauer measurements were carried out in transmission mode on a constant acceleration spectrometer with an Si-PIN semiconductor detector (XR-100CR, AMPTEK Inc.) and multi-channel analyzer of 1024 channels. A 3.7GBq ^{57}Co/Rh of 4mmϕ in diameter was used as γ-ray source. An ^{57}Fe-enriched iron foil was used as velocity calibrant. The two symmetric spectra were folded and velocity range was ± 4mm/s. Thickness corrections of raw spectra were not done.

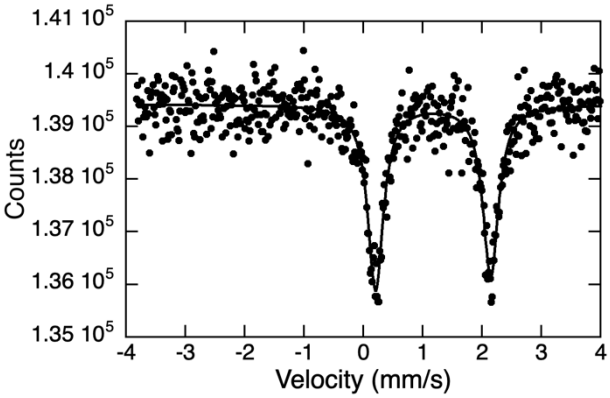

Fig.1. Mössbauer spectrum of diopside measured under γ-ray parallel to the ***a***-axis.

Fig.1 shows Mössbauer spectrum of diopside measured under incident γ-ray parallel to ***a***-axis. A doublet due to Fe^{2+} in *M*1 site of diopside was observed. Averages of isomer shift (δ), Q-splitting (Δ), and line width (Γ) were 1.176(2) 1.919(4) and 0.310(4) mm/s, respectively. From eight sets of intensity of quadrupole doublet, Four components (I_{XX}, I_{YY}, I_{ZZ}, I_{XY}) of the intensity tensor of Fe^{2+} in the *M*1 site of diopside are obtained as 0.328(7), 0.480(5), 0.692(12) and 0.050(15).

DISSCUSSION: The four components (I_{XX}, I_{YY}, I_{ZZ}, I_{XY}) of this study were compared with those of Ca-rich pyroxenes of different chemical compositions in Fukuyama et al. (2022) [2]. According to Fukuyama et al. (2022), the intensity tensor due to Fe^{2+} at the *M*1 sites of diopside, hedenbergite, and augite is dependent on the Wo content, but independent of the Fs content. This result suggests that components of the intensity tensor due to Fe^{2+} at *M* sites in Ca-Mg-Fe pyroxene minerals that contain equal Wo and different Fs components are almost constant.

REFERENCES

[1] Fukuyama., Master thesis, Osaka City Univ. (2020).
[2] D. Fukuyama *et al.,* J. Mineral. Petrol. Sci., **117(1)** (2022) 220506.

PR3-2 Electrical conductivity and the iron valence state of silicate glasses up to Mbar pressures

I. Mashino, T. Yoshino, S. Kitao[1], T. Mitsui[2], R. Masuda[3], M. Seto[1]

Institute for Planetary Materials, Okayama University
[1]Institute for Integrated Radiation and Nuclear Science, Kyoto University
[2]Synchrotron Radiation Research Center, Kansai Photon Science Institute, Quantum Beam Science Research Directorate, National Institutes for Quantum and Radiological Science and Technology
[3]Graduate School of Science and Technology, Hirosaki University

INTRODUCTION: The existance of gravitationally stabilized melts at the bottom of the Earth's mantle has been proposed because a density crossover between melts and crystals is expected to occur. However, whether the crossover occurs in the lower mantle or not strongly depends on the chemical composition of both the melt and crystals. The valence and spin states of iron are believed to affect the iron partitioning between melts and crystals, thus also control a depth of the density crossover [1]. In order to understand the valence/spin states of iron in silicate melts, we firstly conducted high-pressure electrical conductivity measurements of iron-bearing enstatite glass which has a representative composition of the mantle, because silicate glasses have been considered as good analogues of silicate melts.

EXPERIMENTS: ^{57}Fe-bearing enstatite glasses with variable amounts of iron (13 mol% Fe, 19 mol% Fe, and 10 mol% Fe, Al) were synthesized from reagent MgO, $^{57}Fe_2O_3$ and SiO_2 powders by an electric furnace. The conventional ^{57}Fe-Mössbauer spectroscopy was performed using a ^{57}Co source in Rh matrix with nominal activity of 1.85 GBq at Institute for Integrated Radiation and Nuclear Science, Kyoto University. The velocity scale is referenced to α-Fe. To determine the $Fe^{3+}/\Sigma Fe$ and confirm recoilless fractions of Fe^{2+} and Fe^{3+} in the enstatite glasses, we obtained the spectra both at room temperature and at low temperature (22-25 K).

RESULTS: According to the Mössbauer spectroscopy, iron in the enstatite glasses was found to be present as shown in Table 1. Compared with hyperfine parameters in silicate glasses previously reported at ambient condition [2, 3], doublets can be associated with Fe^{3+} or Fe^{2+} in octahedral site.

The ratio of the absorption areas of Mössbauer doublets produced by Fe^{3+} and Fe^{2+} ($A\,(Fe^{3+})_T$, $A\,(Fe^{2+})_T$) are related to the abundances of the ions ($N(Fe^{3+})$, $N(Fe^{2+})$) and the recoilless fraction (f_T) of each ion, according to

$$\frac{A\,(Fe^{3+})_T}{A\,(Fe^{2+})_T} = C_T \frac{N(Fe^{3+})}{N(Fe^{2+})},\ C_T = f(Fe^{3+})_T / f(Fe^{2+})_T, \quad (1)$$

Fig. 1 shows the comparison of Fe^{3+}/Fe^{2+} ratios of Fe-enstatite glasses at room temperature (300 K) and low temperature (22K or 25 K), suggesting that a correlation factor, C_{RT}/C_{LT} is higher than 1. The similar tendency has been observed in previous study on silicate glasses [4].

In-situ high-pressure synchrotron Mössbauer spectroscopic experiments and electrical conductivity measurements have been performed for the Fe-bearing enstatite glasses in a diamond anvil cell. We observed the trend changes in the pressure dependence of electrical conductivity and also the shape changes in Mössbauer spectra at around 80-100 GPa. We are now discussing the obtained results and then geophysical implications.

Table 1. Fitting results of the conventional Mössbauer spectra of Fe-enstatite glasses at ambient pressure.

Sample	Temp. (K)	IS (mm/s)	QS (mm/s)	Width (mm/s)	Aria (%)	Site
13 mol% Fe-enstatite glass						
doublet 1	22	1.19	2.16	0.92	57.3	Fe^{2+}
doublet 2	22	0.49	1.26	0.92	42.7	Fe^{3+}
doublet 3	300	1.05	1.97	0.75	47.7	Fe^{2+}
doublet 4	300	0.36	1.27	0.75	52.3	Fe^{3+}
19 mol% Fe-enstatite glass						
doublet 5	25	1.18	2.18	0.9	45.9	Fe^{2+}
doublet 6	25	0.45	1.25	0.9	54.1	Fe^{3+}
doublet 7	300	1.04	1.98	0.73	39.1	Fe^{2+}
doublet 8	300	0.33	1.22	0.73	60.9	Fe^{3+}
10 mol% Fe, 10 mol% Al-enstatite glass						
doublet 9	22	1.19	2.12	0.91	64.9	Fe^{2+}
doublet 10	22	0.49	1.24	0.91	35.1	Fe^{3+}
doublet 11	300	1.06	1.96	0.75	56.6	Fe^{2+}
doublet 12	300	0.35	1.26	0.75	43.4	Fe^{3+}

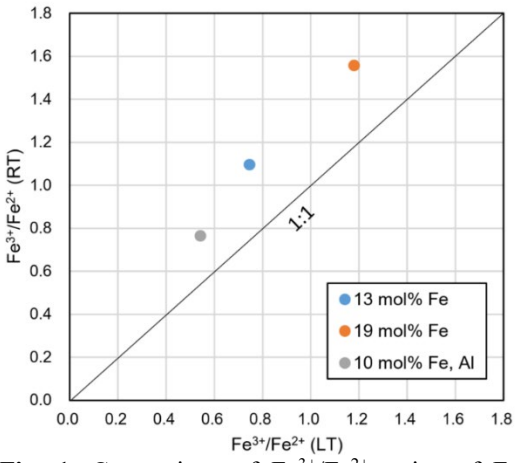

Fig. 1. Comparison of Fe^{3+}/Fe^{2+} ratios of Fe-enstatite glasses at room temperature (RT, 300 K) and low temperature (LT, 22K or 25 K).

REFERENCES:

[1] R. Nomura *et al.,* Nature, **473** (2011) 199.
[2] M. Dyar, Am. Mineral., **70** (1985) 304 .
[3] B. Mysen and P. Richet, Silicate Glasses and Melts (Elsevier, 2019).
[4] H. L. Zhang *et al.,* Chem. Geol., **479** (2018) 166 .

PR3-3 Change in Fe valence state of Fe and Ni substituted Li_2MnO_3 positive electrode material during different synthetic method by ^{57}Fe Mössbauer spectroscopy

M. Tabuchi and Y. Kobayashi[1]

National Institute of Advanced Industrial Science and Technology (AIST)
[1]Institute for Integrated Radiation and Nuclear Science, Kyoto University

INTRODUCTION: The 10% Fe and 20% Ni substituted Li_2MnO_3 ($Li_{1+x}(Fe_{0.1}Ni_{0.2}Mn_{0.7})_{1-x}O_2$, 0<x<1/3) is an attractive positive electrode material having high discharge voltage (>3.5 V) and capacity (>200 mAh/g). However, further effort is needed to improve the electrochemical performance. In this report, we examine the change in Fe valency and local structure using ^{57}Fe Mössbauer spectra after applying ternary calcination process.

EXPERIMENTS: The sample was prepared by co-precipitation - calcination method. Water soluble Fe, Ni and Mn salts (Fe:Ni:Mn molar ratio=1:2:7) dissolved in distilled water and dripped into NaOH solution at +20°C for 2-3 h. The coprecipitate was oxidized by bubbling with O_2 flow for 2 days.

The product was washed with distilled water and then was filtered to make precursor. The precursor mixed with Li_2CO_3 (Li/(Fe+Ni+Mn)=2) into distilled water to make homogeneous slurry. The dried slurry was used as a starting material for calcination. The precursor was powdered using vibration mill and then was primary calcined at 650 °C for 5 h in air. The product was milled again and secondary calcined at 900 °C for 1h in N_2 flow. As a final calcination process, powdered sample was calcined at 450 °C for 3 h in 4%H_2-96%N_2 flow (ternary calcination process). The product was washed with distilled water and then continue to the filtration and drying processes. The obtained sample was named as sample HN. For comparison, the sample was prepared separately by secondary calcination at 900 °C for 10 h in N_2 flow. The sample name was sample N after washing with distilled water and drying processes.

The samples were characterized by X-ray diffraction (XRD), chemical analysis and half-cell tests. The lithium metal foil and 1.5 M Li PF_6/EC-DMC (3:7 in volume) were used as anode and electrolyte, respectively. The velocity axis of each ^{57}Fe Mössbauer spectrum was calibrated by α-Fe.

RESULTS: The X-ray diffraction pattern for both samples showed that each of them consisted of a single phase of monoclinic Li_2MnO_3 type structure. The 5th charge and discharge capacities corresponded to initial specific capacity, because stepwise-charging protocol until 5th cycle was applied to activate this material. The 5th charge and discharge capacities for Li/sample HN cell (267 and 257 mAh/g) were higher than those (242 and 241 mAh/g) for Li/sample N cell. To find the origin of the difference in the electrochemical performance, ^{57}Fe Mössbauer spectroscopy was used. Fig. 1 shows that ^{57}Fe Mössbauer spectra for samples N and HN.

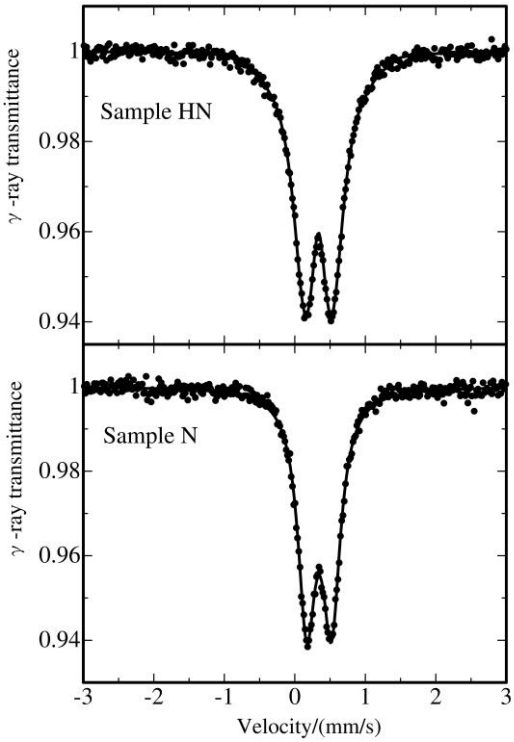

Fig. 1. ^{57}Fe Mössbauer spectra for samples N and HN.

The observed isomer shift (IS) values for samples N and HN were +0.3442 (10) and +0.3362 (10) mm/s, respectively. The Fe valency was assigned as the high-spin trivalent state from the IS data. The fact indicates that trivalent Fe ion was not reduced after calcination in the H_2-N_2 atmosphere. The QS value for the sample HN was 0.43 (3) mm/s, which was larger than that for sample N (0.3522 (17) mm/s). In general, QS value tend to large with increasing variation of local structure. The X-ray Rietveld analysis indicate that transition metal (TM) ion ordering was destroyed on TM-Li layer and part of TM ion in TM-Li layer moved to Li layer for sample HN. The TM distribution disordering was one of origin for larger QS value.

From the ^{57}Fe Mössbauer data, increase in variation of local structure around Fe^{3+} ion is one of important strategy for maximizing of specific capacity for $Li_{1+x}(Fe_{0.1}Ni_{0.2}Mn_{0.7})_{1-x}O_2$, (0<x<1/3) positive electrodes.

PR3-4 Research on magnetism and electronic phase in a H-doped iron-based superconductor

Y. Kamihara, T. Kawamatsu, M. Matoba, S. Kitao[1], and M. Seto[1]
Department of Applied Physics and Physico-Informatics , Faculty of Science and Technology, Keio University
[1]Institute for Integrated Radiation and Nuclear Science, Kyoto University

Superconductivity is a property of conductors, which is confirmed by two properties: zero electrical resistivity below its transition temperature (T_c) and the Meissner effect, which completely eliminates magnetic flux in the conductor.

The performance of power cables using superconductors (SC wire) is determined by the critical current density (J_c), the upper critical magnetic field (H_{c2}), and the irreversible magnetic field (H_{irr}) at the operating temperature below T_c. Here, H_{irr} is the magnetic field defined as the threshold value at which the magnetic flux entering the conductor is unpinned and begins to move due to the application of a magnetic field to the superconductor. In general, the irreversible magnetic field is smaller than the upper critical field. Under a magnetic field larger than the irreversible magnetic field, the zero resistance of the superconductor disappears. In other words, the upper limit of the performance of SC wire is determined by J_c at T below T_c and H below H_{irr}.[1]

Among iron-based high-Tc superconductors (Fe-SC), the J_c of materials with Tc above 20 K can be measured only under the extreme high magnetic field, which is difficult to realize in an ordinary laboratory.[2]

Among the Fe-SC, $SmFeAsO_{1-x}F_x$ (F-doped Sm1111) and $SmFeAsO_{1-x}H_x$ (H-doped Sm1111), whose mother compound is an antiferromagnetic (AFM) metal SmFeAsO, exhibit T_c ~55 K under ambient pressure. [3]

This feature is similar to an electronic and magnetic phase diagram for high-T_c cuprate superconductors, whose mother compound exhibit antiferromagnetic phase of copper sublattice.

Fe ions in SmFeAsO, which is a mother compound of a Fe-SC, exhibit AFM phase at $T < 150$ K. By partial substitution of about 4.5 at.% fluorine or hydrogen at the oxygen sites, the AFM phase disappears and a bulk superconducting phase appears.

At a phase boundary between the superconducting and normal-conductive phases with fluorine or hydrogen atoms around 4.5 at.%, the bulk magnetic phase almost disappears in Sm1111. [4]

However, in this state, local spin density waves (SDW), which indicate a magnetic order at short distances, may exist in a coexisting or phase-separated phases with SC phase. In the case of Sm1111 with higher concentration of fluorine or hydrogen, coexistence or phase separation of SDW and superconducting phase at short range is expected to be realized under high magnetic field.

Focusing on the formation of superconducting electron pairs (Cooper pairs) at the phase boundary between the superconducting and normal-conducting phases under a magnetic field.

The phase boundary in Sm1111 is expected to exhibit a special mechanism of superconducting electron pair formation and destruction, so-called Fulde–Ferrell–Larkin–Ovchinnikov (FFLO) phase. []

In this study, we will demonstrate T_c, J_c, H_{irr}, and Mössbauer spectra under magnetic field for H-doped Sm1111, whose chemical composition has been quantitatively analyzed. Our research aim to define the FFLO state, which exists as a concept, for H-doped Sm1111 experimentally.

EXPERIMENTS: The research in 2022 is the first year of a three-year plan to clarify the bulk electrical and magnetic properties of polycrystalline H-doped Sm1111 prepared by high temperature and high pressure synthesis as a preliminary step for Mossbauer spectroscopy in 2023. The magnetic moment (M) of polycrystalline H-doped Sm1111 was measured using a SQUID magnetometer (Quantum Design MPMS) at several temperatures (T) and magnetic fields (H).

RESULTS: The magnetic moment (M) of polycrystalline H-doped Sm1111 was measured using a SQUID magnetometer (Quantum Design MPMS) at several temperatures (T) and magnetic fields (H).
The magnetic Jc of H-doped SmFeAsO was quantified from the hysteresis of M-H curves using an extended Bean model. [7] The magnetic J_c of our H-doped Sm1111 is 22.3 kA/cm^2.

REFERENCES:

[1] M. Sato, Ph.D. Thesis, Seikei Univ. (2018) (in Japanese).
[2] M. Fujioka, Ph. D thesis, Keio Univ. (2012) (in Japanese).
[3] Y. Kamihara *et al.,* New J. Phys. **12** (2010) 033005.
[4] Y. Kamihara *et al.,* American Physical Society March Meeting, Dallas, USA (2011). (unpublished)
[5] P. Fulde and R. A. Ferrell, Phys. Rev. **135** (1964) A550 .
[6] A. I. Larkin and Yu. N. Ovchinnikov, Sov. Phys. JETP., **20** (1965) 762.
[7] E. M. Gyorgy *et al.,* Appl. Phys. Lett. **55** (1989) 283.

PR3-5 Experimental Preliminary Approach on the Precipitation Mechanism of Banded Iron Formation (BIF): Part 2.

K. Yonezu, H. Hirano[1], K. Arisato[1], Y. Kobayashi[2] and T. Yokoyama[3]

Department of Earth Resources Engineering, Faculty of Engineering, Kyushu University
[1]Department of Earth Resources Engineering, Graduate School of Engineering, Kyushu University.
[2]Institute for Integrated Radiation and Nuclear Science, Kyoto University
[3] Department of Chemistry, Faculty of Sciences, Kyushu University

INTRODUCTION: Banded Iron Formation (BIF) is chemically precipitated sedimentary rock at Precambrian age. Currently iron resource widely used in our industries largely depends on BIF. The formation of BIF was closely related with seafloor hydrothermal activity. In addition, the hydrothermal water, anoxic water was mixed with oxic seawater (e.g., Otake and Otomo, 2021). However, there are many mysteries on the formation mechanism. One of the biggest issues are the alternation of iron mineral and silicate (+carbonate) minerals. Therefore, this study aims to understand the formation mechanism, especially redox condition during the formation of BIF. Here, we would like to report the chemical state of iron in siliceous deposit from geothermal power plant to elucidate the precipitation behavior of iron-bearing siliceous deposit in natural system.

EXPERIMENTS: The siliceous deposit samples used here were collected from operating geothermal power plant. These samples are so called silica scale, and those were analyzed by XRF, XRD, XAFS, NMR in addition to Mossbauer analysis.

RESULTS: Five of silica scale samples were analyzed by Mossbauer spectrophotometry. Those were directly precipitated from geothermal water. Iron concentration in geothermal water is below detection limits of ICP-AES (less than 0.01 ppm), while iron concentration as Fe_2O_3 in silica scale were up to 15% (Tab. 1). This fact suggested that iron is specifically concentrated during silica scale formation.

Iron bearing components observed from the samples were hematite (shown as red in Tab. 2), magnetite/maghemite (shown as orange for A site and pink for B site), goethite (shown as green), iron silicate (shown as purple and blue) and ferric iron (shown as water blue). Sample 1 and Sample 4 shows a similar characteristic from Mossbauer analysis. In addition, those have relatively lower iron and high aluminum contents. Sample 3 consists of the same iron components with Sample 1 and Sample 4, however the ratio of each component is quite different. Sample 3 contains more ferric component than ferrous one. This might be related to high magnesium contents in the sample and the formation of smectite. In contrast, Sample 2 and Sample 5 clearly contain iron oxide, hematite and magnetite/maghemite and goethite.

Tab. 1. Chemical composition of silica scale used in this study.

	Unit	Sample 1	Sample 2	Sample 3	Sample 4	Sample 5
H2O(-)	%	0.0	5.4	2.5	3.8	0.9
H2O(+)	%	15.5	8.3	7.6	9.2	8.6
Fe2O3	%	0.2	12.0	12.3	4.8	15.6
Al2O3	%	12.9	7.0	6.6	10.5	9.3
Na2O	%	1.6	0.8	0.6	1.4	1.4
K2O	%	1.8	0.7	0.3	1.2	1.2
CaO	%	4.5	2.5	1.4	2.3	3.7
MgO	%	0.4	10.5	18.9	7.0	1.7
SiO2	%	75.3	55.6	49.1	70.2	67.3

Tab. 2. Mossbauer parameters obtained from 5 silica scale samples. Cell colors correspond to the component.

	Ratio	IS (mm/s)	Hin (T)	QS (mm/s)	FWHM (mm/s)
Sample 5	11.8%	0.374	51.5	-0.216	0.289
	15.4%	0.308	49.1	-0.053	0.441
	10.5%	0.648	45.9	0.008	0.405
	21.0%	0.238	35.0	-0.420	1.518
	13.1%	1.128		2.614	0.392
	28.2%	0.346		0.720	0.525
Sample 3	29.8%	1.130		2.579	0.365
	26.0%	0.351		0.708	0.430
	44.2%	0.374		1.325	0.532
Sample 2	11.8%	0.369	51.5	-0.208	0.261
	17.8%	0.291	49.0	-0.025	0.373
	21.7%	0.659	45.9	0.007	0.452
	10.4%	0.292	35.6	-0.275	1.674
	13.6%	1.130		2.594	0.394
	24.6%	0.325		0.664	0.460
Sample 4	58.1%	1.106		2.627	0.381
	13.9%	0.308		0.705	0.354
	28.0%	0.475		1.049	0.531
Sample 1	57.0%	1.107		2.616	0.406
	19.8%	0.308		0.705	0.354
	23.2%	0.475		1.049	0.531

Sample 5 is considered to be formed more oxidizing condition based on the ratio of A site and B site. This is also supported by the higher ration of goethite in this sample. By NMR analysis of Sample 5 suggested the presence of only 4-coordinated aluminum and zeolite like structure, while Sample 2 shows the presence of 6-coordinated aluminum suggesting that smectite group mineral harmonious with high magnesium contents.

The formation of silica scale is not monotonous but iron speciation reveals the redox condition of geothermal fluid. In geothermal fluid from geothermal power plant, there are several redox conditions derived from the mixing with oxidizing fluid and/or exposed to atmospheric condition in natural system.

We are going to apply iron Mossbauer spectroscopy for artificial BIF under known redox condition to understand the redox condition of the precipitation environment of BIF.

REFERENCES:

[1] T. Otake and Y. Otomo, Shigen-Chishitsu, **71** (2021) 57-73.

PR3-6 ^{61}Ni Mössbauer Spectroscopy for Hofmann-type Supramolecular Bridging Cyanide Complexes

K. KITASE[1], T. KITAZAWA[1,2], Y. DOI[1], Y. KOBAYASHI[3], S. KITAO[3], T. KUBOTA[4] and M. SETO[3]

[1]*Faculty of Science, Toho University*
[2]*Research Centre for Materials with Integrated Properties, Toho University*
[3]*Institute for Integrated Radiation and Nuclear Science, Kyoto University*
[4]*Agency for Health, Safety and Environment, Kyoto University*

INTRODUCTION: The Mössbauer Effect has been found for about 100 nuclear transitions in some 80 nuclides in nearly fifty elements. The technique is a very valuable and helpful tool to the material sciences linking to molecular magnetisms. It is well-known that 3-d block transition metal complexes with d^4-d^7 configuration in an octahedral crystal field have a possibility of SCO between the low spin (LS) and the high spin (HS) state. Octahedral iron(II) SCO systems with $3d^6$ can be transited between the diamagnetic $(t_{2g})^6$ and the paramagnetic $(t_{2g})^4(e_g)^2$ configuration. Hofmann-type structure is one of coordination polymer consist of center metal ion, bridging cyano metalate, and axial ligand molecule. The first Hofmann-type SCO complex was Fe^{II}(pyridine)$_2$Ni(CN)$_4$ reported in 1996 [1]. Many type of Hofmann-type SCO complex was reported [2-8] due to its tunable properties.

EXPERIMENTS: We freshly synthesized three Hofmann-type coordination polymer Fe(Ethyl Isonicotinate)$_2$Ni(CN)$_4$ and Fe(Allyl Isonicotinate)$_2$Ni(CN)$_4$. These complexes were synthesized by direct method.

^{61}Ni Mössbauer source production associated with ^{62}Ni(γ, p)^{61}Co was done using activation with Bremsstrahlung from the Electron beam of the KURNS-LINAC. ^{61}Ni Mössbauer measurements were carried out conventional methods, since the half-life of ^{61}Co is about 100 minutes, about three hours measurements were done for one cycle. For one SCO compound sample, three times cycles are carried out in order to get suitable Mössbauer spectra. All spectra were obtained at 16 K. Ni-14at%V alloy was used for characterizations of velocities.

RESULTS: Fig. 1 and 2 show/ ^{61}Ni Mössbauer spectra of synthesized complexes. Which show singlet peak. The absorbance of these of Hofmann-type complexes is relatively low. This result can be explain that Hofmann-type structure is relatively soft structure. The obtained Mössbauer parameters have relationship with the square planar crystal field of $[Ni(CN)_4]_2$- units. The parameters for two SCO complexes are slightly different due to slightly different Ni(II) environments, indicating environments of Ni(II) ions are associated with those of Fe(II) ions.

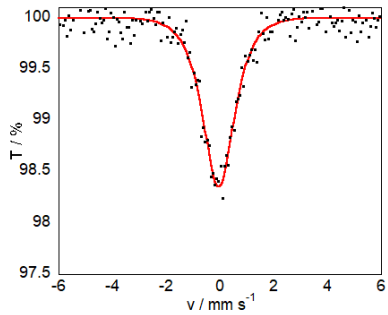

Fig. 1. ^{61}Ni Mössbauer Spectra for Fe(Ethyl Isonicotinate)$_2$Ni(CN)$_4$ (left)

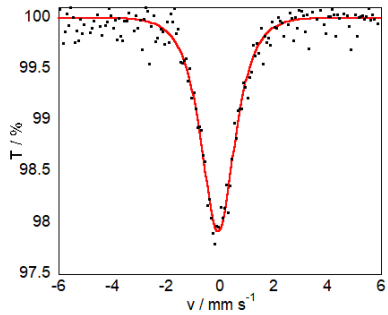

Fig. 2. ^{61}Ni Mössbauer Spectra for Fe(Allyl Isonicotinate)$_2$Ni(CN)$_4$.

REFERENCES:

[1] T. Kitazawa *et al.,* J. Mater. Chem., **6(1)** (1996) 119-121. (doi)10.1039/JM9960600119.
[2] T. Kitazawa, Crystals, **9(8)** (2019) 382. (doi)10.3390/cryst9080382.
[3] K. Kitase *et al.,* Dalton Trans., **52** (2023) 2571-2579. (Back Cover).
[4] K. Kitase *et al.,* Inorg. Chem., **60(7)** (2021) 4717-4722.
[5] K. Kitase and T. Kitazawa, Dalton. Trans., 49 (2020) 12210-12214. (Back Cover).
[6] M. Gábor *et al.,* Chem. Phys. Lett., **423(1-3)** (2006) 152-156.
[7] T. Kitazawa *et al.,* Mol. Cryst. Liq. Cryst. Sci Tech. A, **341**(2000) 527-532. (doi)10.1080/10587250008026193.
[8] T. Kitazawa *et al.,* J. Radioanal. Nucl. Chem., **239(2)** (1999) 285-290. (doi)10.1007/BF02349498.

PR3-7 Chemical species for precursor of supported gold cluster catalysts presumed from Recoil-free fraction in ^{197}Au Mössbauer spectroscopy

H. Ohashi, R. Tawatari, T. Fukae[1], H. Murayama[1], M. Tokunaga[1], Y. Kobayashi[2], S. Kitao[2]

Faculty of Symbiotic Systems Science, Fukushima University
[1]Faculty of Sciences, Kyushu University
[2]Institute for Integrated Radiation and Nuclear Science, Kyoto University

INTRODUCTION:

Though sulfide deposition-precipitation (SDP) method was a kind of new DP method, it was a very unique method and different from DP on several points such as preparation pH. However, until now, the structure of gold sulfide as a precursor synthesized by the SDP method was unknown. ^{197}Au Mössbauer spectroscopy is effective for obtaining information on the precursor.

In previous study, it was estimated that the Debye temperature derived from recoil-free fraction in ^{197}Au Mössbauer spectroscopy for the precursor of heterogeneous gold catalysts by SDP method. In this study, we presumed chemical species for precursor of supported gold cluster catalysts from Recoil-free fraction in ^{197}Au Mössbauer spectroscopy.

EXPERIMENTS:

Gold sulfide (Au_2S_x) and activated carbon supported gold sulfide (Au_2S_x/C) were synthesized by the similar SDP method already reported[1]. ^{197}Au Mössbauer spectra were measured at Kyoto University Research Institute of Nuclear Science. The ^{197}Pt isotope ($T_{1/2}$ = 18.3 h), γ-ray source feeding the 77.3 keV Mössbauer transition of ^{197}Au, was prepared by neutron irradiation of isotopically enriched ^{196}Pt metal at the Kyoto University Reactor. The measurement temperature was 14 - 20 K, and the measurement was performed by the transmission method.

RESULTS:

The ^{197}Au Mössbauer spectra for gold foil (standard) and precursor of supported gold cluster catalysts were measured. These spectra were normalized by the content of gold (n) in measured sample. Each area (A) of normalized spectrum was calculated. There is a following relationship between recoil-free fraction (f) and area;

$$f = a\,A/n \quad \text{(eq.1)}$$

where "a" is proportional constant in this measurement equipment.

No peaks were shown in ^{197}Au Mössbauer spectrum for Au_2S_x/C this time either. However, normal peaks for Au L_3 edge XAFS were obtained and EXAFS analysis showed the presence of S-Au-S chemical bonds.

Figure 1(a) shows a correlation diagram between the reciprocal of the molecular weight of the gold compound and the recoil-free fraction in the ^{197}Au Mössbauer spectrum presented by Parish [2]. Figure 1(b) shows the relationship between the ln$f$ of the prepared gold catalysts and the reciprocal of the molecular weight. ln$f$ was estimated from the area of ^{197}Au Mössbauer spectrum for each catalyst using the value of the constant "a" in eq (1) estimated in the previous report. Molecular weights were calculated from particle sizes estimated from EXAFS analysis. Comparing Fig.1(a) and (b), the tendency of the plots is similar, suggesting that eq (1) was generally satisfied. Spectral noise of the sample without Mössbauer absorption showed that ln$f$ was below -4.6, and the supported gold species was estimated to have a molecular weight of about 250 (Fig.1(b)). Therefore, this gold species was presumed to be an analogous complex of $[Au(SH)_2]^-$.

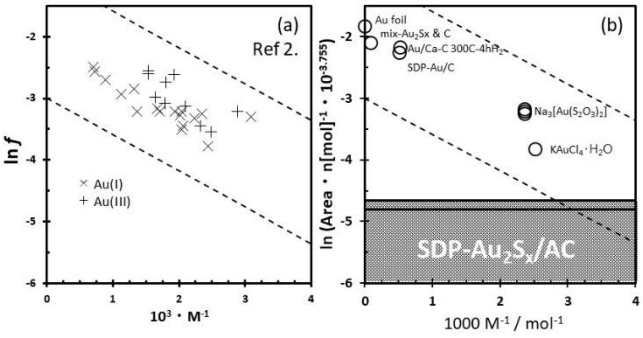

Fig.1.(a) Correlation diagram between the reciprocal of the molecular weight of the gold compound and the recoil-free fraction in the ^{197}Au Mössbauer spectrum [2]. (b) The relationship between the ln$f$ of the prepared gold catalysts and the reciprocal of the molecular weight.

REFERENCE:

[1] H. Ohashi *et al.,* "Method for dispersing and immobilizing gold fine particles and material obtained thereby", Patent No. 5010.

[2] R. V. Parish: in *Modern Inorganic chemistry* by Jolly, W. L, (McGraw-Hill College, 1984) 609-611.

PR3-8 Recoilless Fraction on ^{197}Au Mössbauer Spectroscopy (2)

Y. Kobayashi[1] and H. Ohashi[2]

[1]*Institute for Integrated Radiation and Nuclear Science, Kyoto University*

[2]*Faculty of Symbiotic Systems Science, Fukushima University*

INTRODUCTION: As a study of new materials, we are conducting Mössbauer spectroscopy of Au-supported cat-alysts. When studying the Au catalyst prepared by the calcination of Au compounds, the ratio of each component is important. In the Mössbauer spectra, the spectral ab-sorption area appears as the product of the component ratio of each state and the recoilless fraction. In the ^{57}Fe Mössbauer spectra, the difference in recoilless fraction due to the chemical form of Fe is not significant in most cases. However, in the ^{197}Au Mössbauer spectra, the recoilless fraction is known to differ between Au^{1+} and Au^{3+} [1]. In addition, it is considered that the recoilless fraction be-comes small when the Au metal becomes tiny particles [2]. As the basic data for Au Mössbauer measurements, we measured the absorption area of the spectra in multiple chemical states.

Measuring the absolute amount of the recoilless fraction is difficult due to the background fluctuations in the ^{197}Au Mössbauer measurement. Therefore, we investigated a method for estimating the Debye temperature from the temperature dependence of the spectral absorption inten-sity and confirmed its validity.

EXPERIMENTS: ^{197}Au Mössbauer measurement was conducted using a constant-acceleration spectrometer with a NaI scintillation counter. The ^{197}Au γ-ray source (77.3 keV) was obtained from ^{197}Pt (half-life; 18.3 hours) generated by neutron irradiation to 98%-enriched ^{196}Pt metal foil using KUR. The γ-ray source and samples were cooled to the same temperatures using a helium refrigerator. We prepared Au metal, $Au(OH)_3$ as Au^{3+} and Au_2S as Au^{1+} for measuring sample. The isomer shift value of a gold foil was referenced to 0 mm/s.

RESULTS: Figure 1 shows the Mössbauer spectra of Au_2S at each temperature. Although the counts of the respective spectra are different, the vertical axis ratio is the same. The absorption areas on the spectra decrease at higher temperatures, indicating that the recoilless fraction decreases. Figure 2 shows the temperature dependence of the absorption area on the Mössbauer spectra of each sample. The absorption areas are normalized by the value at 20K. The lines are the calculated value from the equation using each Debye temperature. The absorption areas are proportional to the product of the recoilless fraction of the γ-ray source and the absorber. The Debye temperature of the g-ray source is 270K, which is the Debye temperature of platinum metal.

The temperature dependences of the absorption areas of Au metal and $Au(OH)_3$ are almost the same and agree with the calculated value at the Debye temperature of 164K. 164K is the reported Debye temperature of Au metal. On the other hand, the absorption areas of Au_2S decrease at lower temperatures, which agrees with the calculated value at the Debye temperature of 100K. This result suggests that $Au(OH)_3$ and Au_2S significantly differ in lattice binding strength.

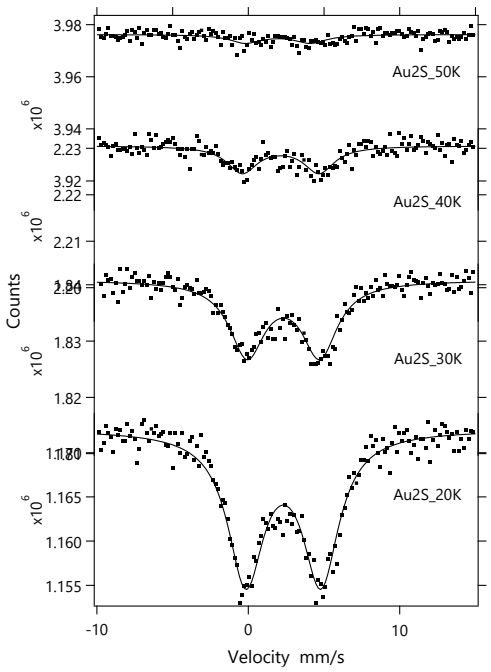

Fig. 1. Mössbauer spectra of Au_2S at each temperature. The ratio of the vertical axis is the same.

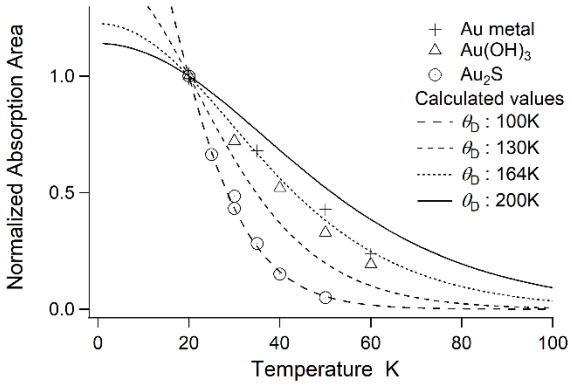

Fig. 2. Temperature dependence of the absorption area on the Mössbauer spectra. The markers are the observed ab-sorption areas (normalized by the value at 20K), and the lines are the calculated values.

REFERENCES:

[1] Jan Stanek, J. Chem. Phys., **76** (1982) 2315.

[2] M. P. A. Viegers and J. M. Trooster, Phys. Rev. B, **15** (1977) 72.

PR3-9 EuS property as the energy standard material at ^{151}Eu Mössbauer spectroscopy

R. Masuda, S. Kitao[1], Y. Kobayashi[1], M. Kurokuzu[1], T. Yamashita[1], and M. Seto[1]

Graduate School of Science and Technology, Hirosaki University
[1]Institute for Integrated Radiation and Nuclear Science, Kyoto University

INTRODUCTION: Mössbauer spectroscopy is usually known as a powerful method for the study of the microscopic state of iron in compounds through the nuclear probe of ^{57}Fe. Despite, there are many other elements the state of which in compounds we can study by Mössbauer spectroscopy. Europium is one of these elements for which we use ^{151}Eu as the probe nuclide. We usually use trifluoride, $^{151}SmF_3$, as the γ-ray source for ^{151}Eu Mössbauer spectroscopy; EuF_3, generated after the β decay of ^{151}Sm in SmF_3, is suitable for the chemical compound for the γ-ray source, because it satisfies almost all the following conditions: i) high recoilless fraction ii) no hyperfine splitting in relating nuclear levels, iii) stability in ambient condition, i.e., the 1 atm, around 300 K, and air atmosphere. Here, the structure of EuF_3 is orthorhombic *Pnma*, thus there might be room for improvement in condition ii), although it is usually sufficiently small in normal study. That is, if we use an alternative chemical specimen with higher symmetry in crystal structure, it might satisfy condition ii) further; that result in the narrow linewidth in instrumental function. In this experiment, we study cubic EuS ($Fm\bar{3}m$) as a candidate for the alternative chemical specimen and measured the temperature dependence of ^{151}Eu Mössbauer spectra to compare the suitability of the specimen as a Mössbauer source.

EXPERIMENTS: The sample was non-enriched EuS purchased from Kojundo Chemical Laboratory Co. Ltd. The purity was 99.9% in the specification sheet. The sample was shaped to the pellet with the cross section of 10 mmφ and the thickness of 43.7 mg EuS/cm^2. The sample was cooled down by a cryostat using Liquid N_2 as the coolant. The Mössbauer spectroscopy was performed at Tracer Laboratory at KURNS. The γ-ray source was $^{151}SmF_3$ at room temperature and the transmitted γ-rays after the EuS sample was detected by Xe proportional counter.

RESULTS: Fig. 1 shows the typical ^{151}Eu Mössbauer spectra of the sample. We can clearly see the signal of EuS as a single-line absorption around the velocity of + 12 mm/s, which indicates Eu^{2+} state in EuS. However, we can also see the other component around +0.7 mm/s, which indicates Eu^{3+} state in this minor component. The area ratio of the minor component is around 15%. We note that the experimental center shift agrees with that of Eu_3S_4 in the literature [1].

Now we focused on the main EuS component. The temperature dependence of the area ratio of the spectra normalized by that at room temperature is shown in Fig. 2. The ratio increased as the temperature of the sample decreased. Because no phase transition is known for EuS between 78 K and room temperature, this change should be due to the recoilless fraction. To estimate the upper limit of the fraction, we estimated the Mössbauer characteristic temperature using the Debye model, ignoring the saturation of the area ratio to the fraction, and obtained that the characteristic temperature is less than 250 K, which corresponds to the recoilless fraction less than 0.544 at room temperature. In the case of this recoilless fraction, the spectral linewidth with the thinnest EuS sample is 1.4 mm/s, which is narrower than the typical experimental linewidth of EuF_3 in ref. 1; that is, EuS might satisfy condition ii) more. Here, we should note that the characteristic temperature of EuF_3 is 283 K [2], and thus the condition i) is less satisfied at EuS.

In summary, EuS might be better than EuF_3 in linewidth, but worse in the recoilless fraction. We will explore further suitable chemical specimens.

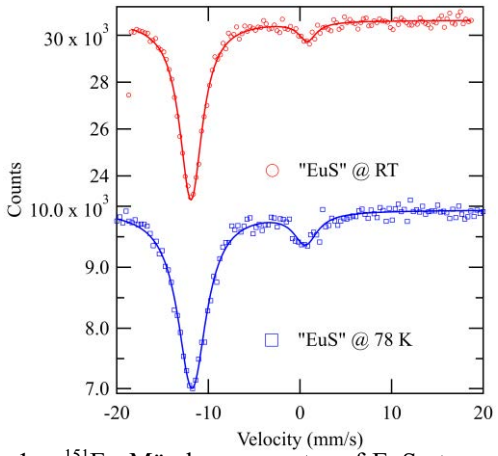

Fig. 1. ^{151}Eu Mössbauer spectra of EuS at room temperature and 78 K.

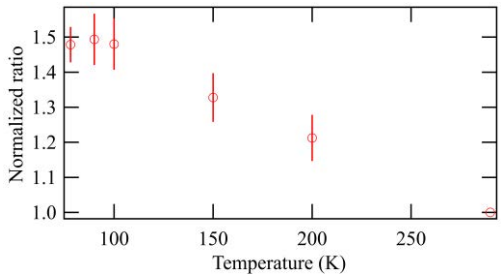

Fig. 2. Temperature dependence of the EuS component in Mössbauer spectra, normalized by that at room temperature.

REFERENCES:

[1] E. R. Bauminger *et al.*, in Mössbauer Isomer Shifts edited by G. K. Shenoy and F. E. Wagner, (North-Holland, Amsterdam, 1978).
[2] C. I. Wynter *et al.*, Hyperfine Interact. **166** (2005) 499-503.

PR3-10 Development of ^{119}Sn Mössbauer Source

S. Kitao[1], Y. Kobayashi[1], M. Kurokuzu[1], T. Kubota[2], H. Tajima[3], H. Yamashita[3], H. Ota[3], R. Masuda[4], and M. Seto[1]

[1]*Institute for Integrated Radiation and Nuclear Science, Kyoto University (KURNS)*

[2]*Agency for Health, Safety, and Environment, Kyoto University*

[3]*Graduate School of Science, Kyoto University*

[4]*Faculty of Science and Technology, Hirosaki University*

INTRODUCTION:

The Mössbauer spectroscopy is one of the most powerful methods to investigate electronic states and magnetic properties by extracting the information of a specific isotope[1]. Mössbauer spectroscopy in general is performed for quite limited isotopes, such as ^{57}Fe and ^{119}Sn. This is partly because only ^{57}Co source for ^{57}Fe and ^{119m}Sn source for ^{119}Sn are commercially available at present. On the contrary, the neutron irradiation facility at Kyoto University Reactor (KUR) at KURNS can be used to product various radioactive isotopes(RIs) for the Mössbauer sources. Moreover, some RIs can be complementarily produced by high-energy γ-ray irradiation converted from electron beam from the electron linear accelerator (KURNS-LINAC). We have been developing practical methods for Mössbauer spectroscopy for various isotopes. Available Mössbauer isotopes at present are as follows (source nuclides in parentheses): ^{61}Ni(^{61}Co), ^{125}Te(^{125m}Te), ^{129}I(^{129}Te,^{129m}Te), ^{161}Dy(^{161}Tb), ^{166}Er(^{166}Ho), ^{169}Tm(^{169}Er), ^{170}Yb(^{170}Tm), ^{197}Au(^{197}Pt), etc.

Although the ^{57}Co and ^{119m}Sn sources are commercially available, it becomes important to produce these sources by ourselves, because these sources are mainly produced in Russia and the international affairs concerning Russia is unstable recently. Therefore, we have been developing a practical production method of ^{57}Co and ^{119m}Sn Mössbauer sources using KUR and KURNS-LINAC.

In this report, an attempt for ^{119m}Sn source production for ^{119}Sn Mössbauer spectroscopy is described. The ^{119m}Sn with a half-life of 293.1 d can be produced by long-term neutron irradiation of ^{118}Sn. As a source material, several compounds are practically used, but degradation by some radiation damage of these compounds by neutron irradiation is unclear. It is necessary to establish a practical production method suitable for the facility at KURNS.

EXPERIMENTS AND RESULTS:

Among several source materials, an attempt with a typical source material, $CaSnO_3$ was studied. The neutron irradiation was performed at long-term irradiation plug of KUR nominally for 12 weeks, which has a net irradiation time of 425 h for 1 MW operation and 84 h for 5 MW operation. Since a natural Sn contains ^{118}Sn with an abundance of 24.23 %, natural Sn was used for this experiment. The $CaSnO_3$ powder was pelletized with Al powder. In order to reduce shorter lived by-product RIs, the irradiated source has used after waiting for a few months from the end of irradiation. The obtained nominal activity of ^{119m}Sn by using 100 mg of Sn was about 880 kBq after 1 month waiting. Since natural Sn contains a number of stable isotopes, several by-product RIs were produced with the neutron irradiation. Short-lived by-products such as ^{117m}Sn with a half-life of 13.6 d, ^{125}Sn with 9.6 d were reduced by waiting for a few months. However, some long-lived by-products such as ^{113}Sn with 115.1 d, ^{123}Sn with 129.2 d remained. Even though these long-lived RIs remained, the Mössbauer γ-rays with the energy of 23.9 keV from ^{119m}Sn can be separated from the γ-rays from other radioactive by-products. The main concern is how to separate Sn KX-rays with energies of around 25 keV to improve measurement efficiency, which cannot separate well by proportional counters or scintillation counters.

Figure 1 shows ^{119}Sn-Mössbauer spectrum of $BaSnO_3$ absorber using obtained $CaSnO_3$ source. The Mössbauer sources are required to be a single-line spectrum with a narrow linewidth. However, the spectrum of irradiated $CaSnO_3$ has not showed a single-line shape. It is possibly because the radiation effect in the $CaSnO_3$ occurs in the irradiated sample and different electronic states appeared in the spectrum. The experiment shows the natural Sn can be used to produce ^{119m}Sn RI source. The radioactive effect from other by-product RIs was not crucial. However, the source material for irradiation and the production method needs to be improved.

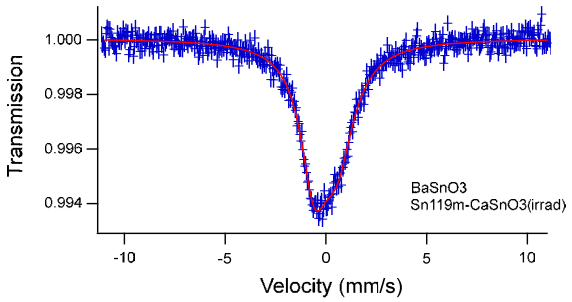

Fig. 1. ^{119}Sn-Mössbauer spectrum of $BaSnO_3$ using ^{119m}Sn source in $CaSnO_3$ at room temperature.

In summary, it is confirmed that ^{119}Sn Mössbauer spectroscopy can be performed by a ^{119m}Sn source obtained by neutron irradiation of natural Sn. However, further improvement of the source material and measurement efficiency must be required for a practical spectroscopy.

REFERENCES:

[1] "Mössbauer Spectroscopy" N. N. Greenwood and T. C. Gibb (Chapman and Hall, London, 1971).